State-selective measurements and calculations of dielectronic recombination with Li-like N^{4+}, F^{6+}, and Si^{11+} ions

L. H. Andersen, G-Y. Pan,* and H. T. Schmidt
Institute of Physics and Astronomy, Aarhus University, DK-8000 Aarhus C, Denmark

M. S. Pindzola and N. R. Badnell
Department of Physics, Auburn University, Auburn, Alabama 36849
(Received 30 December 1991)

Absolute measurements and calculations of the rate coefficient $\langle v\sigma \rangle$ for dielectronic recombination associated with Li-like ions of nitrogen, fluorine, and silicon are reported. The measurements were performed with a single-pass merged-beam technique. The excitation associated with the dielectronic recombination reaction is $2s \rightarrow 2p$. With the present energy resolution, we are able to distinguish between capture into low-lying resonances, which are insensitive to perturbing fields, and capture into the high Rydberg states, which are perturbed by small electric fields present in the experiment. The experimental data are compared with distorted-wave calculations that include the influence of static electric fields in the interaction region.

PACS number(s): 34.80.Kw

I. INTRODUCTION

The process of dielectronic recombination (DR) involves an inverse Auger process. The initially free electron is captured to an ion under the formation of a doubly excited state which decays by emission of photons. The DR process can be represented by

$$X^{q+} + e^- \rightarrow (X^{(q-1)+})^{**} \rightarrow (X^{(q-1)+})^{*} + h\nu \ . \quad (1)$$

If the core-excitation energy for the $2s \rightarrow 2p$ transition considered in the present paper is ΔE and the initial kinetic energy of the electron in the ion rest frame is E_e, then for capture resulting in the population of the $2pnl$ state, energy conservation yields a series of DR resonances at the energy defined via

$$E_e = \Delta E - E_{nl} \geq 0 \ , \quad (2)$$

where E_{nl} is the binding energy of the resonance state designated nl. From Eq. (2), it is seen that for small excitation energies (ΔE), DR results in a series of resonances at low energy (E_e). In particular, when $E_e \approx \Delta E$, very high Rydberg resonances are populated.

The cross section for dielectronic recombination into an isolated resonance $2pnl$ embedded in a single continuum may be written as

$$\sigma_{nl} = \sigma_0 2(2l+1) \frac{A_a(2pnl) A_r(2pnl)}{A_a(2pnl) + A_r(2pnl)} \ , \quad (3)$$

where σ_0 is a proportionality constant and $2(2l+1)$ is the statistical weight of the intermediate state. A_a and A_r are the autoionization decay rate and radiative decay rate, respectively. The first step in the DR process is an inverse Auger process, the probability of which is proportional to A_a. The second step is the radiative stabilization which happens with a probability given by $A_r/(A_a + A_r)$. The Auger and the stabilizing radiative decay may happen via several channels, and the cross-section calculation must include a sum over partial decay rates [not included in Eq. (3)]. The radiative stabilization is normally due to the transition of the core when the final state involves a high Rydberg state. Then A_r is nearly independent of the angular momentum of the Rydberg electron l. For a given n, A_a strongly decreases with increasing l. When, as is often the case for low values of l, $A_a \gg A_r$, it is seen from Eq. (3) that $\sigma_{nl} \propto 2(2l+1) A_r(2pnl)$. For high values of l, $A_a \ll A_r$, and the cross section is negligibly small. Thus we define a critical value of the angular momentum of the Rydberg electron l_c where $A_a(2pnl_c) \approx A_r(2pnl_c)$. All levels with $l < l_c$ contribute to the DR process, and levels with $l > l_c$ may to a first approximation be neglected. The effect of an external electric field is to "tune" more l states of a given n manifold into the DR reaction by mixing low- and high-l states [1]. For high-n states, there are numerous states with $l > l_c$, which in the absence of an external field do not contribute to the DR cross section. In the presence of an external perturbing field these states mix with the low-l states of the same n manifold. Some of these high-l states may obtain an autoionization rate A_a which is larger than or comparable to the radiative decay rate A_r and thus contribute to the DR process. For low-n states, on the other hand, $A_a > A_r$ for all l sublevels and the entire n manifold contributes to the DR process. In this case, the effect of the external electric field is small.

With the present energy resolution, we are able to distinguish between capture to the very high Rydberg states ($n \approx 20$–40) and to states with moderate values of n (≈ 5–10). This enables us to make a comparison between theory and experiment for these high Rydberg resonances which are sensitive to perturbing electric fields present in

the experiment, and at the same time compare theory and experiment for the lower resonances which are field insensitive.

Historically, the importance of l mixing in DR was first recognized by Burgess and Summers [2] who treated the redistribution of the excited-state population as a consequence of collisions. Some years later, Jacobs, Davis, and Kepple [3] used the Stark-broadening theory to calculate DR with highly charged Fe ions and found that the static electric field of the surrounding charged particles could produce an enhancement of the DR cross section.

The first direct measurements of DR appeared in the early 1980s (for a review see, e.g., the comment by Belic and Pradhan [4]). In these studies, core excitations like $2s \rightarrow 2p$ of C^+ [5], N^{2+}, O^{3+}, and F^{4+} [6], C^{2+}, N^{3+}, O^{4+}, and F^{5+} [7], B^{2+}, C^{3+}, N^{4+}, and O^{5+} [8], $3s \rightarrow 3p$ of Mg^+ [1,9] and P^{4+}, S^{5+}, and Cl^{6+} [10], and $4s \rightarrow 4p$ of Ca^+ [11] were considered. They were all associated with rather small excitation energies ΔE and consequently, mainly high Rydberg states were populated. When compared with available theory, it was generally found that the experimental DR cross sections were about a factor of 2 to 10 larger than the calculations. This discrepancy was ascribed to the presence of small static electric fields in the experiments [12]. In most of the experiments, it was rather difficult to predict precisely the electric field produced, e.g., by the space charge of the electron beam. The experiment by Müller *et al.* on Mg^+ [1] was an exception. Here the electric field was known, and in fact, the data and theory were in reasonable agreement for a field of 7.2 V/cm. For 23.5 V/cm, however, the experiment exceeded the theory in some n regions by about 40%.

From the previous work by Dittner *et al.* with Li-like ions [8], it was found that experimental data were in excess of the distorted-wave independent-resonance approximation theory by Griffin, Pindzola, and Bottcher [13] even with full mixing in the calculation. In an earlier paper [14], we reported on DR measurements with Li-like C^{3+} and O^{5+} with much improved energy resolution. Here it was found that the C^{3+} Rydberg contribution was in agreement with the theory by Griffin, Pindzola, and Krylstedt [15] if a field of about 3–4 V/cm was assumed to be present in the experiment. With O^{5+}, the field needed to account for the experimental data at the Rydberg peak was more than 7 V/cm. In the experiment, the field was believed to be in the order of a few volts per centimeter, yet no precise values were given. The overall agreement with theory below the Rydberg peak was for C^{3+} good except for one DR peak close to zero energy. For O^{5+}, the overall agreement was also good. Yet, for some intermediate DR resonances ($n \approx 10-15$) the theory exceeded the experimental O^{5+} data by about a factor of 2.

In the present study, we have continued the experimental and theoretical investigations of DR and Li-like ions and address the important, and to some extent still unsolved, question about the influence of static external electric fields on DR.

II. EXPERIMENT

The present experiment was carried out at the EN tandem accelerator at the Institute of Physics and Astronomy, Aarhus University. Details of the experiment (see Fig. 1) have been published before [14], and only a short description will be given here. We do, however, include a separate discussion on the presence of electric fields in the interaction region. The experiment was based on merging beams of electrons and highly charged ions. The two beams were merged over a section of about 1 m. After the merging region, the electron beam was deflected, and the current was measured with a Faraday cup. The ion beam was focused and charge-state analyzed by passage through a strong electric field. The main beam was measured with a Faraday cup and ions, which have picked up one electron, were detected by a position-sensitive channel-plate detector, the efficiency of which was known from independent measurements.

Instead of cross sections, we determined a quantity

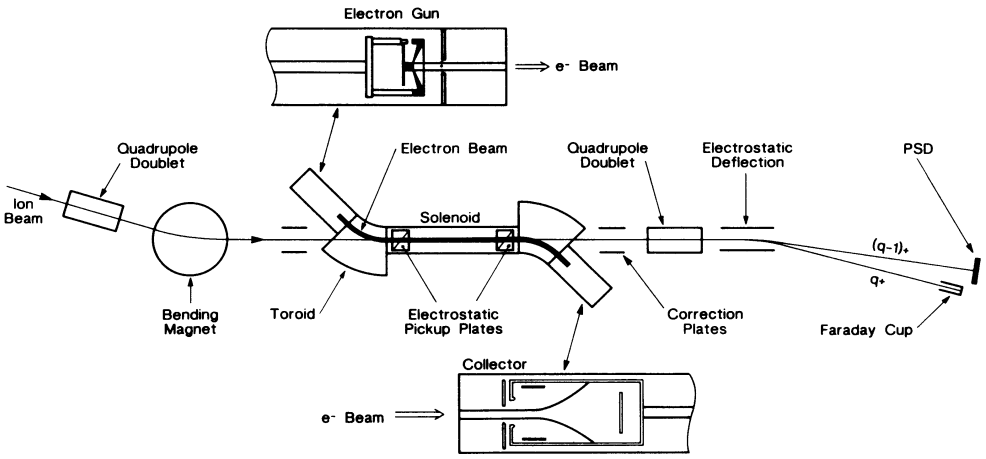

FIG. 1. The experimental setup.

$\langle v\sigma \rangle$ which has the same dimensions as a rate coefficient (cm^3/s):

$$\langle v\sigma \rangle = \frac{N^{(q-1)} - N_0^{(q-1)+}}{N^{q+}} \frac{v_i}{L\rho\varepsilon} , \quad (4)$$

where q is the charge of the incoming ion, L is the length of the interaction section, ε is the ion-detection efficiency, v_i is the ion velocity, and ρ is the electron density which typically was $5\times10^7/cm^3$. $N^{(q-1)+}$ is the total number of ions with charge $(q-1)$, $N_0^{(q-1)+}$ is the background contribution from capture in the rest gas, and N^{q+} is the number of incoming beam particles. Throughout this paper we refer to $\langle v\sigma \rangle$ as a "rate coefficient."

The ion flight time from the interaction region to the charge-state analyzer is about 200 ns. This is shorter than the radiative lifetime of some of the Rydberg states. Thus the strong charge-state analyzing field of about 10 kV/cm used in the experiment prevents some long-lived Rydberg states from contributing to the DR signal. The maximum n, which survives the analyzer field, is given approximately as

$$n_{max} = (6.2\times10^8 q^3/E)^{1/4} , \quad (5)$$

where E is the electric field strength in V/cm [16].

There is a slight potential shift across the electron beam due to the space-charge potential. The space-charge potential from the nearly uniform electron beam may, inside the electron beam, be written as

$$V_s = K(r)\frac{I_e}{\sqrt{E_e}} , \quad (6)$$

where r is the radial position in the electron beam, I_e the electron current in mA, and E_e the electron energy in the laboratory frame in eV. The function $K(r)$ in V is

$$K(r) = 15.14\left[\left[\frac{r}{a}\right]^2 - 1 + 2\ln\left[\frac{a}{R}\right]\right] , \quad (7)$$

where a is the electron-beam radius (0.5 cm) and R is the radius of the surrounding vacuum tube (5 cm). Assuming a Gaussian ion-beam profile of width 2σ, displaced by r_0 from the center of the electron beam, we obtain the following approximation of the average electric field produced by the space charge in V/cm:

$$\bar{E} = \frac{I_e}{a^2\sqrt{E_e}}(24\sigma e^{-1/2(r_0/\sigma)^2} + 30r_0) , \quad (8)$$

where σ, a, and r_0 are in centimeters. In deriving Eq. (8), we have ignored any space-charge neutralization by ions trapped in the electron beam. From the observed positions of our DR resonances, we know that this effect is small. From Eq. (8) it is seen that for a finite ion-beam width, there is an electric field, perpendicular to the beam direction, acting on the ions in the interaction region even for $r_0=0$. For a typical measurement, $2\sigma=0.2$ cm, $I_0=10$ mA, and $E_e=850$ eV. This yields a field of about 3 V/cm for $r_0=0$. The field becomes 6 V/cm for $r_0=0.1$ cm. With the electrostatic pickup plates mounted inside the interaction region (see Fig. 1), it was easily verified that the ions moved inside the electron beam, the diameter of which was 1.0 cm. It was difficult with the ion-beam intensities of about 1 μA, used in the present work, to determine r_0 to a precision better than 0 ± 0.1 cm. Thus, the uncertainty in the prediction of the space-charge field resulting from the uncertainty in the determination of the ion-beam position is about 3 V/cm. The width of the ion beam 2σ was determined from an ion-optics simulation program and measured with a Faraday probe at the exit of the interaction region. The uncertainty of the space-charge field stemming from the uncertainty of the ion-beam width (±0.1 cm) is less than 2 V/cm.

When an ion moves in a magnetic field transverse to its direction of motion, an electric field in the center of mass is produced. The strength is

$$E' = \gamma\beta c B_\perp , \quad (9)$$

where $B_\perp$ is a magnetic-field component perpendicular to the beam direction. β is the ion speed divided by the speed of light v_i/c, and γ is the $(1-\beta^2)^{-1/2}$ [17]. In the experiment, the ions are moving with a relatively high velocity of about 5% of the speed of light. From the ion-optics simulation program, we get an average divergence of the ion beam which is about 1.7 mrad (calculated for 20 MeV O^{5+}). With a solenoid field of 150 G, this yields an average magnetic field perpendicular to the ion-beam direction of 0.26 G. This results in an electric field of approximately 4 V/cm in the ion frame. Depending on the position and angle of the ions relative to the center of the electron beam, this field may add to the space-charge field or partly cancel it.

III. THEORY

In the isolated-resonance approximation, the energy-averaged dielectronic recombination cross section for a given initial level i through an intermediate level j is given by [18]

$$\bar{\sigma}(i\to j) = \frac{2\pi^2}{\Delta\varepsilon k^2}\frac{g_i}{2g_j}\frac{A_a(j\to i)\sum_k A_r(j\to k)}{\sum_h A_a(j\to h) + \sum_h A_r(j\to h)} . \quad (10)$$

The above equation is in atomic units and $\Delta\varepsilon$ is an energy bin width larger than the largest resonance width, k is the linear momentum of the continuum electron, g_j is the statistical weight of the $(N+1)$-electron doubly excited level, and g_i is the statistical weight of the N-electron target level. First-order many-body perturbation theory is used to evaluate both the radiative A_r and the autoionization A_a rates for the many intermediate levels j in the energy range of interest.

To evaluate Eq. (10), we made use of the previously written computer code DRFEUD [13] which calculates intermediate-coupled single-configuration dielectronic-recombination cross sections for low n explicitly and for high n by extrapolating matrix elements of the dipole-radiative and electron-electron Coulomb interactions. In

the presence of an external electric field, the doubly excited levels for each n are constructed from the matrix diagonalization of a Hamiltonian which includes Stark l-mixing effects. These field-mixed levels are then used to calculate radiative and autoionizing rates which, in turn, provide a field-dependent dielectronic-recombination cross section. We ignore mixing between different n states, and the effects that the electric field may have on the continuum electron. Explicit correlation effects, such as core polarization, have not been included in the calculation.

For dielectronic recombination in Li-like ions we consider the following reaction pathways:

$$\begin{aligned} 1s^2 2s + e^- &\rightarrow 1s^2 2pnl \rightarrow 1s^2 s + e^- \\ &\rightarrow 1s^2 2p + e^- \\ &\rightarrow 1s^2 2snl + h\nu_1 \\ &\rightarrow 1s^2 2pn'l' + h\nu_2 \ . \end{aligned} \tag{11}$$

The first decay channel for the $2pnl$ resonance configuration is related to the capture channel by the principle of detailed balance. The second decay channel depends on the $2p(J=\frac{1}{2})$ to $2p(J=\frac{3}{2})$ core splitting and is available only for relatively high n values in low-charged ions. The third decay channel is usually stronger than the fourth for low-charged ions. The calculation includes final states with $n \leq n_{\max}$, where $n_{\max}$ was calculated according to Eq. (5).

In order to compare the theory with the experimental data, we calculated

$$\begin{aligned} \langle v\sigma \rangle &= \int_0^\infty \sigma(E) \left[2\frac{E}{m} \right]^{1/2} \frac{dN}{dE}(E)dE \\ &= \sum_i \sigma_{\varepsilon_0, \Delta\varepsilon^i} \int_{(i-1)\Delta\varepsilon}^{i\Delta\varepsilon} \left[2\frac{E}{m} \right]^{1/2} \frac{dN}{dE}(E)dE \ , \end{aligned} \tag{12}$$

where dN/dE is the electron density which is given in terms of the relative velocity distribution $f(v)$:

$$\frac{dN}{dE} = \frac{v}{m} \int_\Omega f(v) d\Omega \ . \tag{13}$$

Due to the longitudinal acceleration of the electron beam, the relative velocity spread in the experiment cannot be characterized by a single temperature. The velocity distribution was characterized by a product of two Maxwellian distributions, one accounting for the transverse electron motion, and one for the longitudinal motion. The velocity distribution then becomes

$$f(v) = \frac{m}{2\pi k T_\perp} e^{-m v_\perp^2 / 2kT_\perp} \left[\frac{m}{2\pi k T_\parallel} \right]^{1/2} e^{-m(v_\parallel - \Delta)^2 / 2kT_\parallel} \ , \tag{14}$$

where $v_\perp$ and $v_\parallel$ are the electron-velocity components perpendicular and parallel to the ion-beam direction, respectively, and Δ is the detuning velocity that defines the relative energy ($\frac{1}{2}m\Delta^2$). It was found that the measured shape of individual DR resonances contains information which could easily yield the transverse energy spread $kT_\perp$ as well as the longitudinal energy spread $kT_\parallel$. The two temperatures were $kT_\perp = 0.15$ and $kT_\parallel = 0.001$ eV. In some instances, a modulated electron beam was used to better subtract the background contribution. The transverse temperature $kT_\perp$ was then unchanged and $kT_\parallel = 0.002$ eV.

IV. RESULTS AND DISCUSSION

In Fig. 2 we show the experimental data together with the calculation for N^{4+}. The data are presented as the rate coefficient $\langle v\sigma \rangle$ as a function of the relative energy. The $2s \rightarrow 2p$ excitation energy is 10.0 eV where we see a strong contribution due to capture to the high Rydberg states. DR associated with capture into the lower-n states ($n = 5, 6, \ldots$) is also seen. The resonance positions shown in the figure are calculated from the Rydberg formula $E_n = q^2\ (13.6\ \text{eV})/n^2$ and the resonance condition Eq. (2). The overall structure of the spectrum is well described by the theory.

As discussed earlier, the calculated rate coefficient for the Rydberg peak ($n > 15$) will be sensitive to small static electric fields. A field of about 5 V/cm in the distorted-wave calculations is required to account for the observed peak height. To test the dependence on the electric field in the interaction region, we performed a series of measurements of the Rydberg peak at different electron densities, corresponding to an electron-beam current of 5, 7.5, and 10 mA. For the three separate measurements, the ion beam was kept at the same position. The electron beam at each electron current was centered with an accuracy of ± 0.02 cm. Thus, essentially, only the size of the

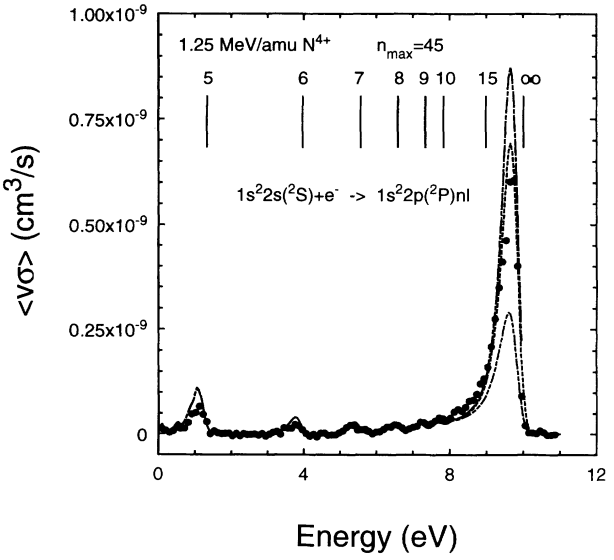

FIG. 2. The rate coefficient $\langle v\sigma \rangle$ as a function of electron energy for 1.25 MeV/amu N^{4+}. Shown are the experimental data together with the calculations including different fields; highest to lowest, 10 V/cm (dashed curve), 5 V/cm (dotted curve), and 0 V/cm (dash-dotted curve). The temperatures $kT_\perp = 0.15$ and $kT_\parallel = 0.001$ eV were used in the calculation of the rate coefficient.

space-charge field was changed. In order to diminish problems with changing electron-beam temperatures, we integrated the obtained rate coefficient from 8.0 to 10.5 eV. The integrated rate coefficient as a function of the calculated space-charge field is shown in Fig. 3. To calculate the field, we assumed a beam width 2σ of 0.2 cm and an ion-beam position r_0 between 0 and 0.1 cm. The horizontal error bars are due to the possible variation in r_0. The vertical error bars correspond to $\pm 15\%$ uncertainty on the absolute scale (one standard deviation). In the calculation of the field, we neglected the possible influence of motionally induced fields E'. The experimental data exceed the theory by about 10%. The data points are slightly above the theory presumably because the experimental rate coefficient at $n \approx 10-15$ exceeds the theory.

In Fig. 4 we show the low-energy part of the N^{4+} spectrum taken with small energy steps. Negative energies correspond to the situation where the electrons are slower than the ions, and positive energies correspond to the case where the electrons are faster than the ions. We find that in this region of energy, both radiative recombination (RR) and dielectronic recombination contribute by a significant amount. To display theory and experiment in one figure, we multiplied the DR theory by 0.6. In general it is quite difficult to predict accurate DR cross sections near threshold since the k^2 factor in the denominator of Eq. (10) magnifies slight errors in the energy positions of the resonance features. We do see, however, several l-resolved resonances from the $2p5l$ configurations. The RR contribution, which peaks at $E_r = 0$, was calculated on the basis of the Kramers hydrogenic formula [19] and the Gaunt corrections [20–22].

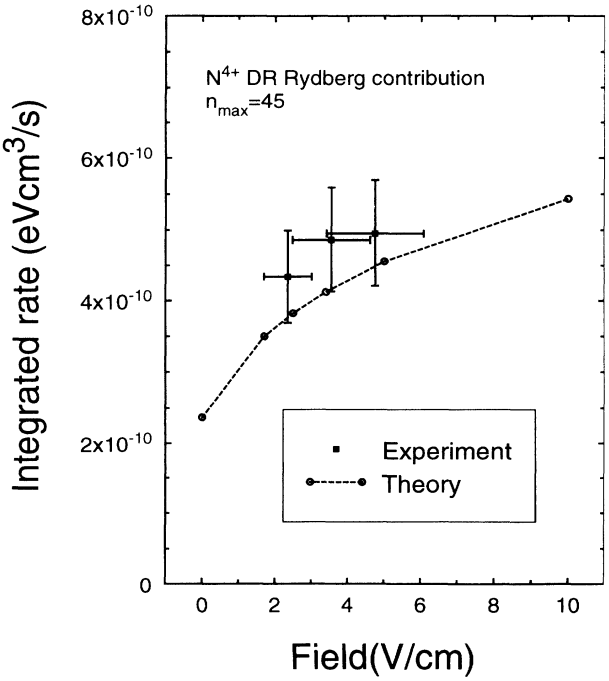

FIG. 3. The experimental and theoretical rate coefficient of the Rydberg contribution for N^{4+} integrated from 8 to 10.5 eV as a function of the calculated space-charge field.

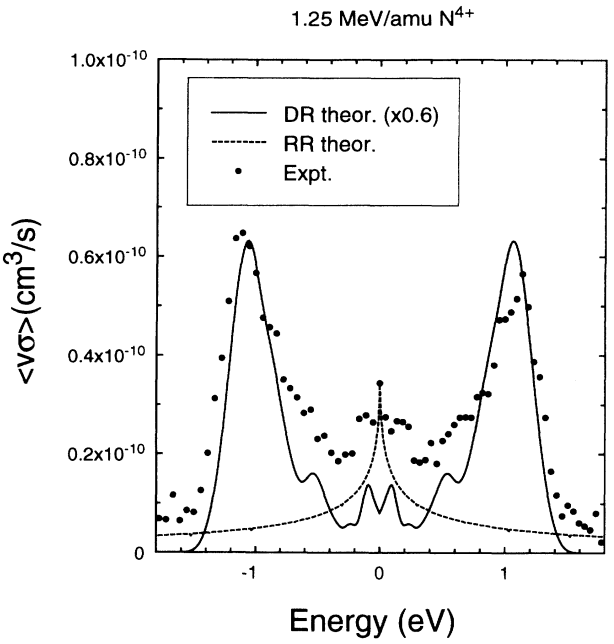

FIG. 4. High-resolution spectrum for N^{4+} obtained for relative energies between 0 and 1.8 eV. The full curve is the present DR calculation multiplied by 0.6. The dashed curve is the calculated RR contribution. In the calculations, we used $kT_\perp = 0.15$ and $kT_\parallel = 0.002$ eV.

As the effective charge in the calculation we used the total ion charge (4). This has earlier been demonstrated to be a good approximation for the Li-like ions [23,24]. We do not expect any significant interference between the

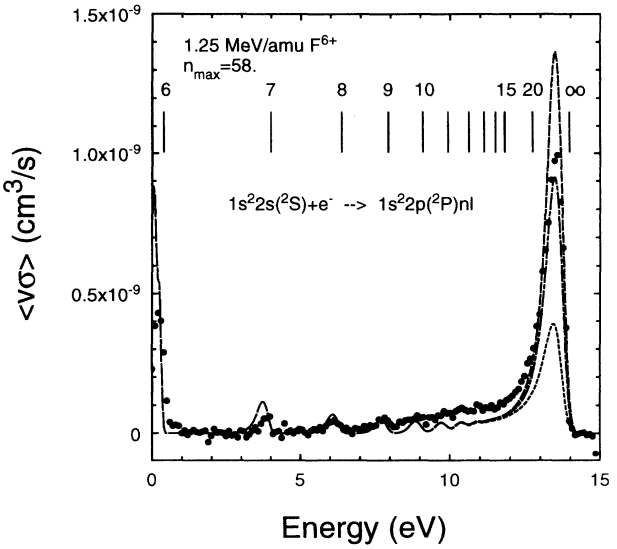

FIG. 5. The rate coefficient $\langle v\sigma \rangle$ as a function of electron energy for 1.25 MeV/amu F^{6+}. Shown are the experimental data together with the calculations including different fields; highest to lowest, 15 V/cm (dashed curve), 5 V/cm (dash-dotted curve), and 0 V/cm (dotted curve). The temperatures $kT_\perp = 0.15$ and $kT_\parallel = 0.001$ eV were used in the calculations of the rate coefficient.

RR and DR recombination channel since only a small fraction of the RR signal results in population of the excited state with $n=5$.

The data and theory obtained with F^{6+} are shown in Fig. 5. Again, there is a good overall agreement between data and theory. However, as for N^{4+}, and C^{3+} [14], the theory seems to overestimate the contribution of the lowest n resonances. The $2p6l$ configurations are found to straddle the threshold, the majority of the $2p6p$ states below, the majority of the $2p6d$ states above. If one shifts the resonance spectrum by 0.15 eV, the DR peak at threshold drops by a factor of 2. The Rydberg peak is accounted for when a field of about 5 V/cm is used in the calculation. The intermediate resonances $n=10$ to 15 are underestimated by about a factor of 2 in the calculation. The same discrepancy was found earlier for O^{5+} [14].

As a last example of DR with Li-like ions, we show in Fig. 6 the data obtained with Si^{11+}. The experimental data are associated with more unfavorable statistics due to a much lower ion-beam current. At low energy (<1 eV), a strong RR signal is observed. The obtained RR-rate coefficient was accounted for by a hydrogenic calculation [24].

Due to the relative low Si^{11+} ion current it was not possible to determine the accurate position of the beam. For Si^{11+}, there is a significant fine-structure splitting between the $J=\frac{1}{2}$ and $\frac{3}{2}$ states. This results in a series of double-peaked resonances in the spectrum. In particular, it is seen that the Rydberg peak is split into two components. The relative height of the double-peaked Rydberg structure is sensitive to the field strength, as demonstrated by the calculation. This gives an independent measure for the field in the interaction region. A field somewhere between 0 and 5 V/cm reproduces the relative height of the two fine-structure peaks. To account for the the total size of the Rydberg peak, however, a field of about 10 V/cm is required in the calculation.

It is possible that part of the observed discrepancy at the Rydberg peak is due to radiative stabilization of the high Rydberg states from above n_{max} to states below n_{max} prior to the charge-state analyzer field. The apparent discrepancy (for Si^{11+}) concerning the electric field in the interaction region would then be due to the neglect of states above n_{max} which may contribute in experiment and not in the calculation rather than an incorrect treatment of the perturbation by the field. The error introduced by the choice of the n_{max} cutoff [Eq. (5)] was evaluated by considering Rydberg states above n_{max} with a lifetime shorter than 200 ns which is the ion flight time from the electron target to the analyzer field. Our analysis showed that many such states exist for Si^{11+}, whereas for N^{4+} and F^{6+} the number was small. However, the short-lived Rydberg states mainly have low-l values. The effect may be limited then, since the zero-field DR cross section for a particular value of n has significant contributions extending to $l=5$ or 6. The effect of the field is to further increase the contribution from the higher-l states. Such high l states, however, do not radiate before the analyzer field.

The apparent discrepancy is probably not due to the neglect of field-induced n mixing and interference between different n manifolds. These effects were evaluated by Harmin [25], who showed that they will result in a reduction of the field enhancement rather than an enhancement.

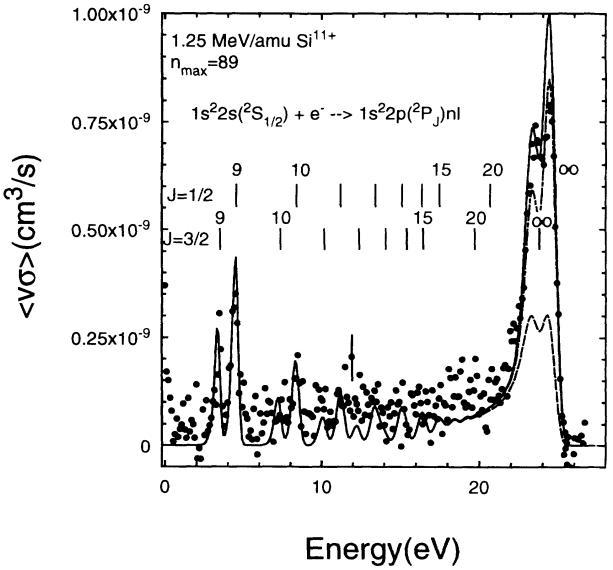

FIG. 6. The rate coefficient $\langle v\sigma \rangle$ as a function of electron energy for 1.25 MeV/amu Si^{11+}. Shown are the experimental data together with the calculations including different fields; highest to lowest, 10 V/cm (full curve), 5 V/cm (dash-dotted curve), and 0 V/cm (dashed curve). The temperatures $kT_{\perp}=0.15$ and $kT_{\parallel}=0.002$ eV were used in the calculation of the rate coefficient. One error bar due to counting statistics is shown.

V. CONCLUSION

The DR rate coefficient for Li-like ions of N, F, and Si has been measured and calculated for the $2s \rightarrow 2p$ excitation. The overall structure of the experimental data is well described by the performed distorted-wave calculations. It is evident, however, that the magnitude of the low DR resonances are difficult to predict by the theory. In order to account for the size of the Rydberg contribution for N^{4+} and F^{6+}, fields in the order of 5 V/cm are needed in the calculation. Our analysis shows that fields of this magnitude are to be expected in the experiment, but we have emphasized that it is generally difficult to predict precisely the actual electric field in the experiment.

For Si^{11+}, a field of about 10 V/cm is required to account for the height of the Rydberg peak. With a field below ≈ 5 V/cm, the calculation reproduces the relative height of the $J=\frac{1}{2}$ and $\frac{3}{2}$ contributions to the Rydberg peak. We have pointed out that some missing contribu-

tion due to relatively short-lived Rydberg states may explain some of the apparent discrepancy for Si^{11+}. The importance of this effect is not precisely known yet.

We also find that the theoretical prediction for N^{4+}, O^{5+}, and F^{6+} for the lower Rydberg resonances ($n \approx 10-15$), which are essentially unperturbed by the field, is lower than the experimentally obtained rate coefficient.

ACKNOWLEDGMENTS

The experimental work was supported by the Danish National Council of Science, the Ib Henriksen Foundation, and the Carlsberg Foundation, and the theoretical work by the Office of Fusion Energy, U.S. Department of Energy, under Contract No. DE-FG05-86ER53217 with Auburn University.

*Permanent address: Institute of Physics, Chinese Academy of Science, Beijing, People's Republic of China.

[1] A. Müller, D. S. Belic, B. D. DePaola, N. Djuric, G. D. Dunn, D. W. Mueller, and C. Timmer, Phys. Rev. A **36**, 599 (1987).

[2] A. Burgess and H. P. Summers, Astrophys. **157**, 1007 (1969).

[3] V. L. Jacobs, J. Davis, and P. C. Kepple, Phys. Rev. Lett. **37**, 1390 (1976).

[4] D. Belic and A. K. Pradhan, Comments At. Mol. Phys. **20**, 317 (1987).

[5] J. B. A. Mitchell, C. T. Ng, J. L. Forand, D. P. Levac R. E. Mitchell, A. Sen, D. B. Miko, and J. W. McGowan, Phys. Rev. Lett. **50**, 335 (1983).

[6] P. F. Dittner, S. Datz, R. Hippler, H. F. Krause, P. D. Miller, P. L. Pepmiller, C. M. Fou, Y. Hahn, and I. Nasser, Phys. Rev. A **38**, 2762 (1988).

[7] P. F. Dittner, S. Datz, H. F. Krause, P. D. Miller, P. L. Pepmiller, C. Bottcher, C. M. Fou, D. C. Griffin, and M. S. Pindzola, Phys. Rev. A **36**, 33 (1987).

[8] P. F. Dittner, S. Datz, P. D. Miller, P. L. Pepmiller, and C. M. Fou, Phys. Rev. A **35**, 3668 (1987).

[9] P. F. Dittner, S. Datz, P. D. Miller, P. L. Pepmiller, and C. M. Fou, Phys. Rev. A **33**, 124 (1986).

[10] D. S. Belic, G. H. Dunn, T. J. Morgan, D. W. Mueller, and C. Timmer, Phys. Rev. Lett. **50**, 339 (1983).

[11] J. F. Williams, Phys. Rev. A **29**, 2936 (1984).

[12] K. Lagatutta and Y. Hahn, Phys. Rev. Lett. **51**, 558 (1983).

[13] D. C. Griffin, M. S. Pindzola, and C. Bottcher, Phys. Rev. A **33**, 3124 (1986).

[14] L. H. Andersen, J. Bolko, and P. Kvistgaard, Phys. Rev. A **41**, 1293 (1990).

[15] D. C. Griffin, M. S. Pindzola, and P. Krylstedt, Phys. Rev. A **40**, 6699 (1989).

[16] F. Brouillard, in *Atomic and Molecular Processes in Controlled Thermonuclear Fusion,* edited by C. J. Jochain and D. E. Post (Plenum, New York, 1983).

[17] L. Landau and E. Lifshitz, *The Classical Theory of Fields* (Addison-Wesley, New York, 1951).

[18] Y. Hahn, Adv. At. Mol. Phys. **21**, 123 (1985).

[19] H. Bethe and E. Salpeter, *Quantum Mechanics of One- and Two-Electron Systems,* Handbuch der Physik Vol. 35 (Springer, Berlin, 1957).

[20] J. A. Gaunt, Philos. Trans. A **229**, 163 (1930).

[21] D. C. Griffin, Phys. Scr. **T28**, 17 (1989).

[22] L. H. Andersen and J. Bolko, Phys. Rev. A **42**, 1184 (1990).

[23] L. H. Andersen and J. Bolko, J. Phys. B **23**, 3167 (1990).

[24] L. H. Andersen, G-Y. Pan, and H. T. Schmidt, J. Phys. B **25**, 277 (1992).

[25] D. A. Harmin, Phys. Rev. Lett. **57**, 1570 (1986).